Contrib. Astron. Obs. Skalnaté Pleso **50**, 219 – 234, (2020)
https://doi.org/10.31577/caosp.2020.50.1.219

Possible observational signatures of supermassive black hole binaries in their Fe Kα line profiles

P. Jovanović[1,*], V. Borka Jovanović[2], D. Borka[2] and L.Č. Popović[1]

[1] *Astronomical Observatory, Volgina 7, P.O. Box 74, 11060 Belgrade, Serbia*
[*] *(E-mail: pjovanovic@aob.rs)*

[2] *Atomic Physics Laboratory (040), Vinča Institute of Nuclear Sciences, University of Belgrade, P.O. Box 522, 11001 Belgrade, Serbia*

Received: July 10, 2019; Accepted: October 24, 2019

Abstract. Here we study the potential observational signatures of supermassive black hole binaries (SMBHBs) in the Fe Kα line profiles emitted from the accretion disks around their components. We simulated the Fe Kα line emission from the relativistic accretion disks using ray tracing method in Kerr metric. The obtained profiles from the SMBHBs are then compared with those in the case of the single supermassive black holes (SMBHs). We considered two models of the SMBHBs: a model when the secondary SMBH is embedded in the accretion disk around the primary, causing an empty gap in the disk, and a model with clearly separated components, where the accretion disks around both primary and secondary give a significant contribution to the composite Fe Kα line emission of a such SMBHB. The obtained results showed that both models of SMBHBs can leave imprints in the form of ripples in the cores of the emitted Fe Kα line profiles, which may look like an absorption component in the line profile. However, in the case of the composite line profiles emitted from two accretion disks, these ripples could have much higher amplitudes and strongly depend on orbital phase of the system, while for those emitted from a disk with an empty gap, the corresponding ripples mostly have lower amplitudes and do not vary significantly with orbital phase. The present day X-ray telescopes are not able to detect such signatures in the observed X-ray spectra of SMBHBs. However this will be possible with the next generation of X-ray observatories, which will also enable application of such effects as a tool for studying the properties of these objects.

Key words: black hole physics – supermassive black holes – accretion disks – line: profiles

1. Introduction

Nowadays, it is widely accepted that binary systems of SMBHs originate in galactic mergers (Begelman et al., 1980), and that their coalescences are the powerful emitters of low-frequency (nHz) gravitational waves (GWs) which are currently probed by pulsar timing arrays (PTA, Sesana et al., 2018), and which

will be main targets for future space-based interferometers. Searches for (active) SMBHBs are currently ongoing, resulting with more than 100 candidates (see e.g. Sesana et al., 2018, and references therein), and were significantly intensified after the first observation of merging stellar mass black hole binary performed by LIGO Scientific Collaboration and Virgo Collaboration (2016).

One of the most powerful methods for SMBHB searches is the spectroscopy (in different spectral bands). As two SMBHs in a galactic merger become gravitationally bound and start to orbit around their center of mass, the emission lines from SMBH components start to shift due to their radial velocities (see e.g. Popović, 2012; Bon et al., 2012; Li et al., 2016, for examples in optical band). In such a case, a strong X-ray emission in the broad Fe Kα line at 6.4 keV could arise from accretion disks around both SMBHs, and could be therefore affected by the Doppler shifts due to the orbital motion of the binary (Yu and Lu, 2001; Jovanović et al., 2014), since the radial velocities of its components could reach $\approx 1.5 \times 10^4$ km/s in the case when the separation between them is $10^{-3} - 10^{-2}$ pc (see Table 1 in Popović, 2012). Such, double relativistic Fe Kα lines and periodic X-ray variability are expected to be detected from very massive ($M > 10^8\ M_\odot$) and cosmologically nearby ($z_{cosm} < 1$) SMBHBs (Sesana et al., 2012).

The Fe Kα line is produced by fluorescent emission from a very compact region around a SMBH (Fabian et al., 1989, 2000), and thus it represents powerful diagnostic tool for studying physics and structure of such regions (see e.g. Jovanović et al., 2008; Jovanović & Popović, 2009; Jovanović, 2012; Popović, 2012), as well as the masses and spins of SMBHs (see e.g. Jovanović et al., 2011; Reynolds, 2014). X-ray reflection spectroscopy, which is based on the studies of the observed broad Fe Kα line profiles, is nowadays proven to be an especially powerful technique for the robust black hole spin measurements across the wide range of black hole masses, from the stellar-mass black holes in the X-ray binaries to the SMBHs in the Active Galactic Nuclei (AGN), as well as for the reverberation of the relativistically broadened iron line which is already detected in the observed X-ray spectra of some AGN (for more details see the review by Reynolds (2014), and references therein).

In the case of SMBHBs, the line emitting regions could have different structures, depending on the mass ratios of the components, separation between them and parameters of their accretion disks (Jovanović et al., 2014). In some cases the secondary SMBH could be even embedded in the accretion disk around the primary, causing an empty annular gap in it (McKernan et al., 2013), similarly to the empty gap in circumbinary disk of Mrk 231 (see Fig. 1 in Yan et al., 2015). Namely, it is well known that a SMBHB with small mass ratio ($q \ll 1$) can exchange angular momentum with its disk, distorting its density and causing the secondary SMBH to migrate inward (see e.g. McKernan et al., 2013, and references therein). If a secondary has a very low mass, it is subjected to a very rapid Type I migration, and it cannot significantly affect the Fe Kα line emitted form the disk, neither can create an empty cavity in it. However, if the

secondary is sufficiently massive (i. e. if the mass ratio of the SMBHB exceeds the critical value of $q \geq 10^{-4}$), it will be subjected to a Type II migration, and it will open an empty annular gap in the disk, analogous to the gaps in protoplanetary disks, significantly affecting the emitted Fe Kα line (McKernan et al., 2013).

Here we study the possibility to detect the SMBHB signatures in their observed Fe Kα line profiles by nowadays and future X-ray detectors. For this purpose we studied two models of the SMBHBs: (1) model with clearly separated components, where the accretion disks around both primary and secondary SMBHs significantly contribute to their composite line emission, and (2) model in which the secondary SMBH is embedded in the accretion disk around primary, causing an empty gap in the disk.

This paper is organized as follows: the simulations of X-ray radiation from two accretion disks with different parameters, as well as the procedure how to obtain the simulated Fe Kα line profiles for two mentioned models of SMBHBs are described in Section 2, the obtained results are presented in Section 3 and briefly discussed in Section 4, and finally, in Section 5 we point out our main conclusions.

2. Models of accretion disks around two components of a SMBHB and their barycentric orbits

2.1. Accretion disk models

In order to study the potential observational signatures of SMBHBs in the Fe Kα line profiles emitted from the relativistic accretion disks around their SMBH components, we performed the numerical simulations of disk emission based on ray-tracing method in Kerr metric, taking into account only those photon trajectories reaching the observer's sky plane (Fanton et al., 1997; Cadez et al., 1998; Jovanović et al., 2008; Jovanović & Popović, 2009; Jovanović, 2012). We assumed that disk emissivity $\varepsilon(r)$ follows power law: $\varepsilon(r) = \varepsilon_0 \cdot r^p$, where ε_0 is an emissivity constant, and p is an emissivity index (see Jovanović, 2012, for more details). In the case of the SMBHB model with empty gap, this power law disk emissivity was modified so that $\varepsilon(r) = 0$ over the annulus representing the gap (see below text for more details).

Due to several effects, photons emitted from a disk at energy E_{em} (or wavelength λ_{em}) will be observed by an observer at infinity at energy E_{obs} (or wavelength λ_{obs}), causing the energy shift g or, equivalently, the usual redshift in wavelength z (for more details see e.g. Jovanović et al., 2016, and references therein):

$$g = \frac{E_{obs}}{E_{em}} = \frac{\lambda_{em}}{\lambda_{obs}} = \frac{1}{1+z}. \tag{1}$$

By integrating the observed flux at each observed energy over the whole disk image, one can obtain the corresponding simulated line profile emitted from the

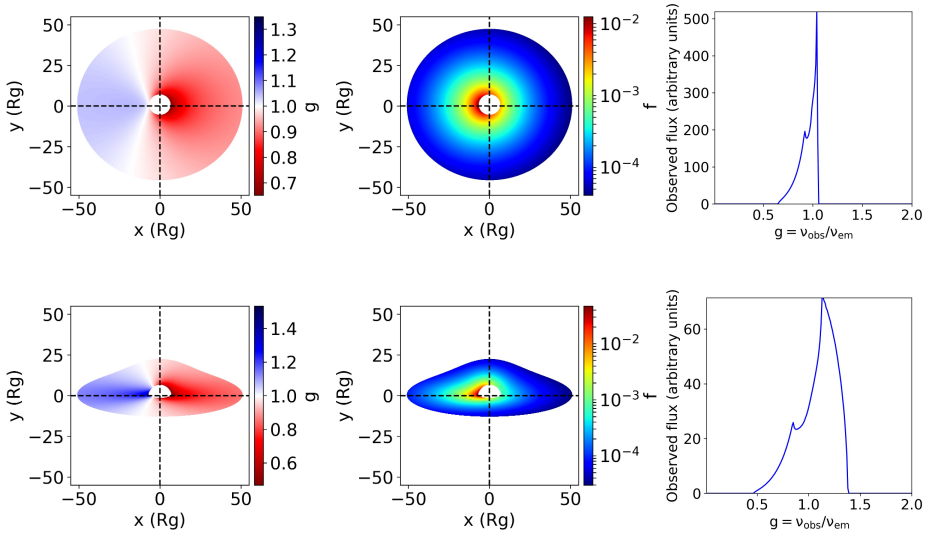

Figure 1. Simulated images of the relativistic accretion disk in Kerr metric around a SMBH, colored according to energy shift g (left) and observed flux (middle), as well as the corresponding simulated non-normalized line profile (right). Top panel corresponds to "disk model A" and bottom to "disk model B" (see §2 for the particular values of disk parameters).

previously calculated accretion disk image (Jovanović, 2012):

$$F_{obs}\left(E_{obs}\right) = \int\limits_{image} \varepsilon\left(r\right) g^4 \delta\left(E_{obs} - gE_0\right) d\Xi \tag{2}$$

Taking into account the results of some previous studies (see e.g. Jovanović, 2012, and references therein), we assumed the following parameters for modeling the accretion disks around the primary and secondary SMBHs: both SMBHs are assumed to be slowly rotating with the same small spin: $a_{BH} = 0.1$, inner radii of both disks are fixed to $R_{in} = R_{ms} = 5.67\,R_g$ (where R_{ms} is the radius of the marginally stable orbit, and $R_g = GM/c^2$ - the gravitational radius of the SMBH with mass M), their outer radii are also assumed to be the same: $R_{out} = 50\,R_g$, as well as their emissivity indices: $p = -2.5$. We simulated the SMBHB signatures for two different disk inclinations: $\theta_{obs} = 25°$ (labeled as "disk model A" for the further reference) and $\theta_{obs} = 75°$ ("disk model B"). The resulting simulated disk images, colored according to the energy shifts g and the observed fluxes F, as well as the corresponding simulated non-normalized line profiles are presented in Fig. 1 for both disk models. As it can be seen from this figure, disk inclination significantly affects the width and intensity of

the resulting line profiles, which was the main reason why we assumed these particular two disk models.

Since, as already mentioned, the appearance of double relativistic Fe Kα lines and periodic X-ray variability are expected to be detected from very massive and cosmologically nearby SMBHBs (Sesana et al., 2012), we assumed a large mass of the primary SMBH: $M_1 = 5 \times 10^8\ M_\odot$ and small angular diameter distance to the binary system of SMBHs: $D_A = 20$ Mpc, corresponding to $z_{cosm} \approx 0.0045$ for $\Omega_M = 0.315, \Omega_\Lambda = 0.685$ and $H_0 = 67.4\ \mathrm{km\,s^{-1}\,Mpc^{-1}}$ (Planck Collaboration, 2018). For mass ratio of the SMBHB we adopted the value $q = 0.5$, corresponding to the mass of the secondary of $M_2 = 2.5 \times 10^8\ M_\odot$. Thus, the total mass of the SMBHB is almost an order of magnitude less than the mass of the central SMBH of M87, estimated from its shadow by Event Horizon Telescope Collaboration (Event Horizon Telescope Collaboration, 2019), and it is within the mass limit of $1.6 \times 10^9\ M_\odot$ for the SMBHBs out to the distance of the Virgo Cluster (≈ 16 Mpc), obtained from 11-year data set for low frequency gravitational waves by NANOGrav PTA collaboration (Aggarwal et al., 2019). This resulted with simulated accretion disk around the primary with outer radii of $R_{out} = 50\ R_g \approx 250$ AU which on the observer's sky corresponds to $\approx 12.5\ \mu$as, giving a total apparent size of the disk's image of $\sim 25\ \mu\mathrm{as} \times 25\ \mu$as.

Regarding the assumed size of the accretion disks, we took into account the results of some observational studies of AGN with single SMBHs in their centers, which suggest that the broad Fe Kα line is emitted from the innermost regions of their accretion disks, extending between R_{ms} and a few dozens of R_g (see e.g. Ballantyne & Fabian, 2005, for an example in the case of radio galaxy 4C 74.26). This is also in accordance with so called "standard model of accretion disk" (Shakura & Sunyaev, 1973), according to which the spectrum of radiation emitted from the disk depends on the distance to the central SMBH, so that the innermost part of the disk between R_{ms} and several tens of R_g emits X-rays, its central part between $\sim 100\ R_g$ and $\sim 1000\ R_g$ emits UV radiation, while its outer part located thousands R_g from the SMBH, emits the optical radiation. Taking this into account, and since we are here investigating only the Fe Kα line emission from a SMBHB, we assumed that the outer radii of its both disks are equal to the outer radii of their Fe Kα line emitting regions, for which we adopted the following value: $R_{out} = 50\ R_g$.

On the other hand, the outer parts of an accretion disk in a close SMBHB (i.e. when semimajor axis a is small), could be subjected to the tidal disruption by the gravitational field of the second component. Therefore, the maximum size of the accretion disks in such a SMBHB is determined by the gravitational interaction between its components, and it is a function of their mass ratio q (for more details see e.g. Paczynski, 1977). An accretion disk with outer radius R_{out} would be tidally disrupted if the semimajor axis a of the SMBHB is less than the following limit for for tidal disruption (Safarzadeh et al., 2019):

$$a_t = R_{out}\left(1 + q^{1/3}\right). \tag{3}$$

In this study, the outer radii of the disks are $R_{out} \approx 250$ AU, which corresponds to the following limit for tidal disruption: $a_t \approx 450$ AU. As it can be seen from Table 1, the semimajor axes of both studied orbits significantly exceed this limit ($a \gg a_t$), and thus the accretion disks around both components are not subjected to the tidal disruption during their orbital motion.

2.2. Keplerian barycentric orbits of SMBHBs

The first of two studied SMBHB models assumes that its clearly separated primary and secondary components are moving around their common center of mass along Keplerian orbits which, due to their radial velocities, causes Doppler shifts in the Fe Kα lines emitted from their accretion disks.

To model Keplerian barycentric orbits of a binary sistem of SMBHs, we apply the same procedure which is commonly used for the binary stars (for more details see e.g. Hilditch, 2001). As a first step, we can adopt some masses of the primary and secondary components M_1 and M_2, or alternatively, just mass of the primary and mass ratio between the secondary and primary: $q = \dfrac{M_2}{M_1}$. We also need to assume some separation between the components a (i.e. semimajor axis of their relative orbit)[1]. The orbital period of the binary can be then obtained from the third Kepler's law:

$$P^2 = \frac{4\pi^2 a^3}{G\,(1+q)\,M_1}. \tag{4}$$

If we denote time with t and time of the pericenter passage with τ, then the next step is to calculate the mean anomaly M (and also orbital phase Φ):

$$M = \frac{2\pi}{P}\,(t-\tau) = 2\pi\Phi. \tag{5}$$

Assuming some orbital eccentricity e, the corresponding eccentric anomaly E can be obtained by solving the Kepler's Equation:

$$M = E - e\sin E, \tag{6}$$

and the true anomaly θ can be calculated from E according to:

$$\theta = 2\arctan\left(\sqrt{\frac{1+e}{1-e}}\tan\frac{E}{2}\right). \tag{7}$$

Finally, the true barycentric orbits (i.e. those in the orbital plane) of the primary and secondary SMBHs are then represented by polar equations of the ellipse

[1]Sub-parsec SMBHBs are of special interest for this investigation, since several observational studies indicated the existence of such SMBHBs in the cores of some AGN (see e.g. Bon et al., 2012).

$r_{1,2}(\theta)$:

$$r_{1,2}(\theta) = \frac{a_{1,2}\left(1-e^2\right)}{1+e\cos\theta}, \tag{8}$$

where $a_1 = \dfrac{q\,a}{1+q}$ and $a_2 = \dfrac{a}{1+q}$ are their semimajor axes[2].

The corresponding apparent orbits (in rectangular coordinates) can be calculated by projecting the true orbits on the observers sky plane using the remaining three Keplerian orbital elements (orbital inclination i, longitude of the ascending node Ω and longitude (or argument) of pericenter ω):

$$\begin{aligned} x_{1,2} = {} & r_{1,2}\cos\theta\left[\cos\Omega\cos\omega - \sin\Omega\sin\omega\cos i\right] \\ & + r_{1,2}\sin\theta\left[-\cos\Omega\sin\omega - \sin\Omega\cos\omega\cos i\right] \\ y_{1,2} = {} & r_{1,2}\cos\theta\left[\sin\Omega\cos\omega + \cos\Omega\sin\omega\cos i\right] \\ & + r_{1,2}\sin\theta\left[-\sin\Omega\sin\omega + \cos\Omega\cos\omega\cos i\right]. \end{aligned} \tag{9}$$

Radial velocities of the components are given by the following expression (Hilditch, 2001):

$$V_{1,2}^{rad}(\theta) = K_{1,2}\left[\cos(\theta+\omega) + e\cdot\cos\omega\right] + \gamma, \tag{10}$$

where $K_{1,2}$ are the semiaplitudes of the velocity curves:

$$K_{1,2} = \frac{2\pi a_{1,2}\sin i}{P\sqrt{1-e^2}}, \tag{11}$$

and γ is systemic velocity (which is assumed to be 0 km/s in our simulations). Assuming that $V_{1,2}^{rad} \ll c$, Doppler shifts in wavelength ($z_{1,2}$) and energy ($g_{1,2}$) due to radial velocities of the components are given by:

$$z_{1,2} \approx \frac{V_{1,2}^{rad}}{c}, \quad g_{1,2} = \frac{1}{1+z_{1,2}}. \tag{12}$$

The total redshift factor g_{tot}, representing the net effect of both relativistic effects and radial velocities of the components, can be then obtained from Eqs. (1) and (12):

$$g_{tot} = \frac{1}{1+z+z_{12}} = \frac{1}{\dfrac{1}{g}+\dfrac{1}{g_{1,2}}-1}. \tag{13}$$

We studied the influence of Doppler shifts on the observed disk emission by calculating the simulated line profiles according to the expression (2), but using the total redshift factor g_{tot} instead of g.

[2]One should also take into account that the orientations of two barycentric orbits differ by 180° within the orbital plane.

Table 1. Adopted orbital elements for two Keplerian orbits of a SMBHB with mass ratio $q = 0.5$.

	a		Period	e	i	Ω	ω
	(AU)	(pc)	(yr)		(°)	(°)	(°)
orbit 1	1×10^3	0.005	1.16	0.5	30	0	30
orbit 2	2×10^3	0.01	3.27	0.25	60	0	90

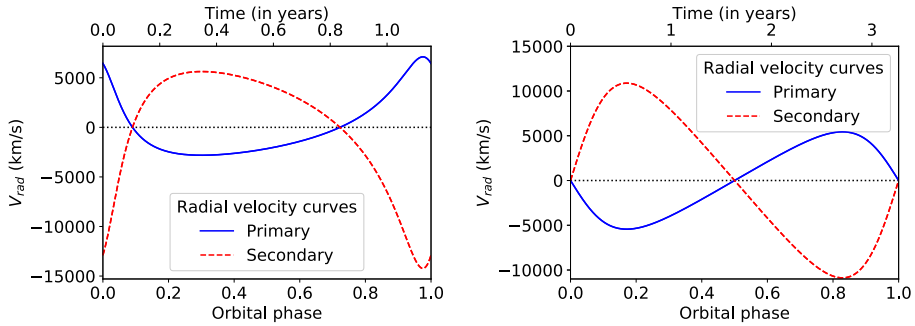

Figure 2. Radial velocities of the components in a SMBHB with mass ratio $q = 0.5$, for orbit 1 (*left*) and for orbit 2 (*right*).

3. Results and discussion

To study the observational signatures of the first SMBHB model, we performed simulations of the X-ray radiation from such a SMBHB with mass ratio $q = 0.5$ for two different Keplerian orbits of its components, denoted as "orbit 1" and "orbit 2", and determined by the orbital elements which are summarized in Table 1. As it can be seen from this table, the obtained orbital periods are on the order of a few years, which means that we simulated electromagnetic signatures in the Fe Kα line of the nearby SMBHBs with semimajor axes of $\sim 10^{-3} - 10^{-2}$ pc, periods of a few years and masses above $\sim 10^8\ M_\odot$, and such SMBHBs are targets of present PTAs like NANOGrav, which search for their gravitational wave signatures (see e.g. Aggarwal et al., 2019).

The obtained radial velocities of the components in the case of both orbits from Table 1 are presented in Fig. 2. It can be seen from this figure that the radial velocity of the secondary SMBH can go far beyond 10,000 km/s, which is sufficient to induce significant Doppler shift in the X-ray radiation from its accretion disk.

As a next step, we used the obtained radial velocities to simulate the X-ray radiation from this SMBHB during different orbital phases along each of two orbits, assuming different models of accretion disks around its components. Two

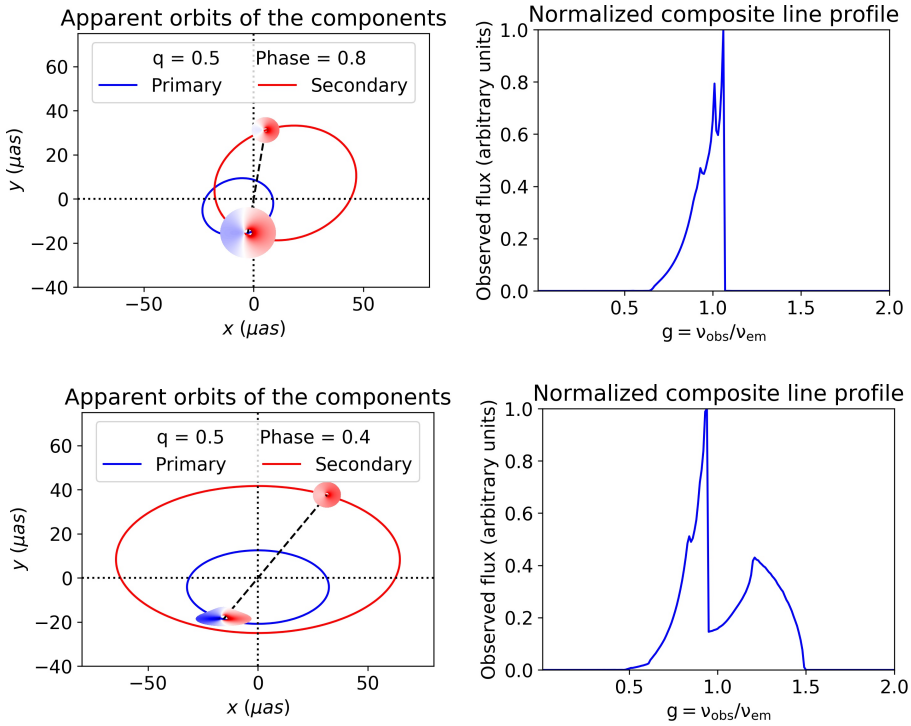

Figure 3. *Left*: Simulated images of the accretion disks around the primary and secondary components of a SMBHB with $q = 0.5$ for "disk A" around both primary and secondary during orbital phase 0.8 along "orbit 1" (*top panel*), as well as for "disk B" around primary and "disk A" around secondary during orbital phase 0.4 along "orbit 2" (*bottom panel*). *Right*: The corresponding simulated composite Fe Kα line profiles.

examples of the obtained results are presented in Fig. 3 and they correspond to the orbital phase $\Phi = 0.8$ along "orbit 1" in the case when "disk A" is around both components (top panel), as well as to the orbital phase $\Phi = 0.4$ along "orbit 2" in the case when "disk B" is around the primary and "disk A" around the secondary component (bottom panel). The disk images, colored according to the total redshift factor g_{tot}, are presented in the left parts of each panel of Fig. 3, while their right parts show the corresponding simulated composite Fe Kα line profiles. As it can be seen from this figure, this model of SMBHB induces the appearance of the ripples in the cores of the simulated composite Fe Kα line profiles. The amplitudes of these ripple effects strongly depend on the assumed parameters of the accretion disks around both primary and secondary SMBHs, the orbital elements of their Keplerian orbits, as well as on the particular orbital phase (i.e. time) at which, here a simulation and in reality an observation, is

made. Moreover, as demonstrated in Jovanović et al. (2014), the mass ratio q also has a strong influence on the amplitudes of these ripples, since the ratio between the fractions of the composite Fe Kα line flux, contributed by the accretion disks around the secondary and the primary, roughly corresponds to q. Since a highly inclined disk produces a wide line profile, as demonstrated in Fig. 1, the ripple in the bottom panel of Fig. 3 is much wider and deeper than the one in the top panel because it is created in the component of the Fe Kα line which is emitted from the highly inclined "disk B" around the primary SMBH.

We also investigated the flux variability in different parts of the Fe Kα line for different phases during one orbital period. The flux variability of the total line profile, its red part ($E < 6.2$ keV), core (6.2 keV $\leq E \leq$ 6.6 keV) and blue part ($E > 6.6$ keV) are presented in Fig. 4 by black, red, green and blue lines, respectively. Two panels in Fig. 4 refer to the same disk parameters and orbital elements as the corresponding panels in Fig. 3, but for 10 different orbital phases (including those from Fig. 3). As it can be seen from Fig. 4, this model of SMBHBs induces the highest flux variability in the core of the Fe Kα line. Taking into account that the presented results refer to only one orbital period, it can be easily deduced that the same variability pattern would also repeat during all successive orbital periods. Therefore, in the case of such a SMBHB, a periodic variability of the X-ray radiation in the Fe Kα line should be expected, which is in good agreement with the similar predictions of Sesana et al. (2012).

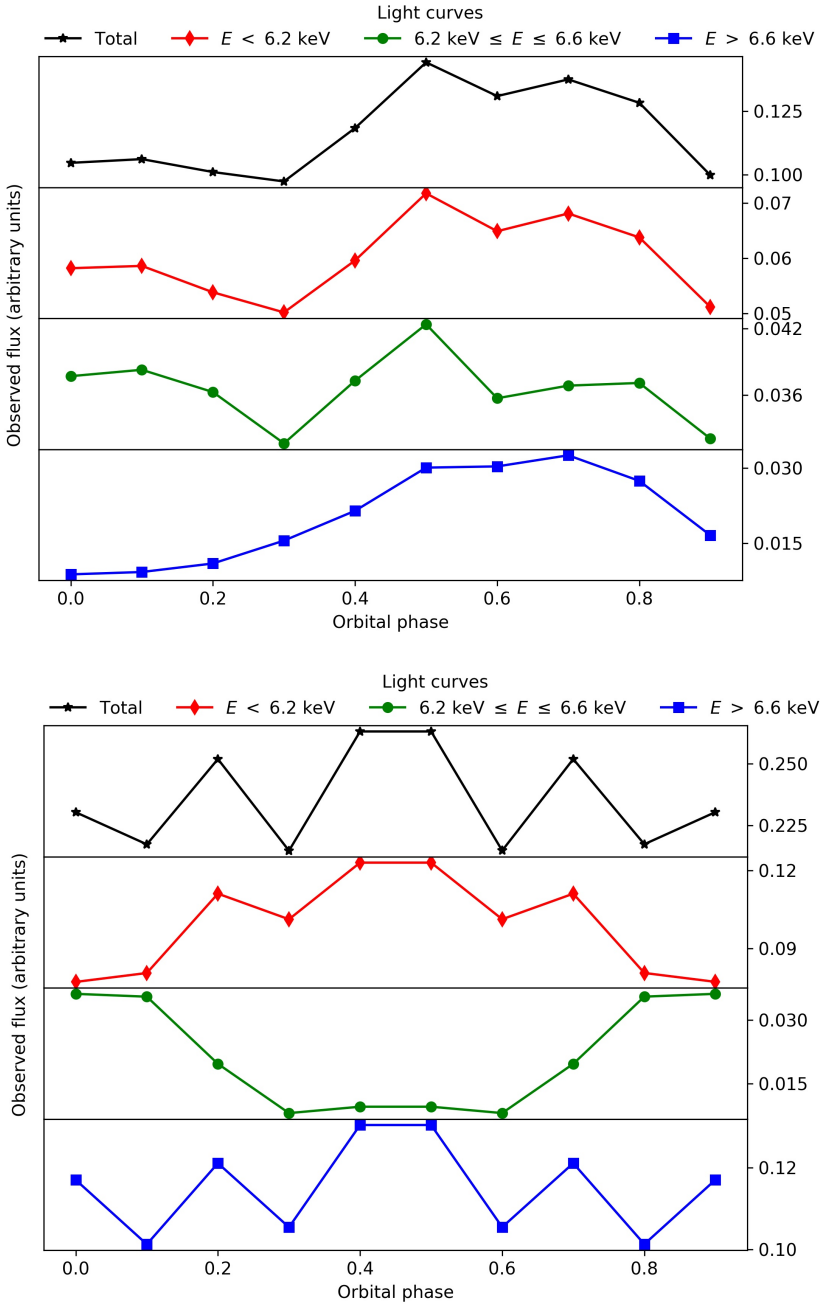

Figure 4. Flux variability (from top to bottom) of the total Fe Kα line profile (black line), its red part (red line), core (green line) and blue part (blue line) during 10 different orbital phases and for the same disk parameters and orbital elements as in the corresponding panels of Fig. 3.

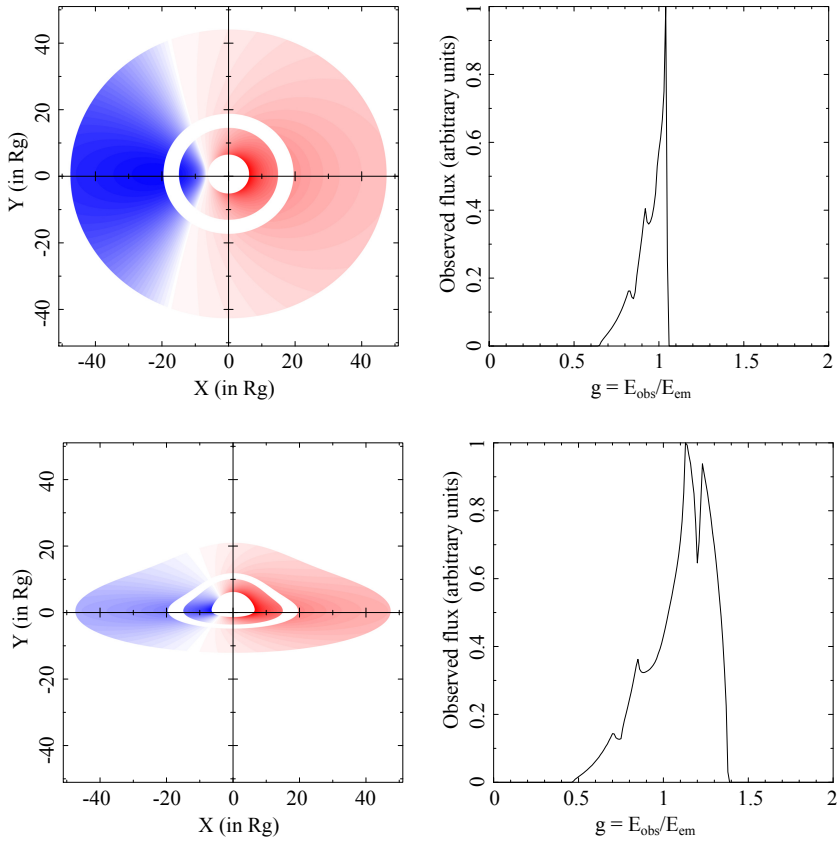

Figure 5. Illustrations of two relativistic accretion disks with an empty gap extending from $15R_g$ to $20R_g$ (*left*), and the corresponding simulated Fe Kα line profiles (*right*). Top panel corresponds to the first, and bottom panel to the second model of accretion disks, as described in §2.

We studied the observational signatures of the second SMBHB model using the similar simulations of the X-ray radiation from the accretion disk around its primary SMBH, in which its secondary SMBH cleared an empty gap. We performed these simulations for both disk models from §2 and for different positions and widths of the empty gap, i.e. for different values of its inner and outer radii. Two examples of the obtained results in the case of "disk A" and "disk B", each with an empty gap extending between 15 R_g and 20 R_g, are shown in the left panels of Fig. 5, while the corresponding simulated Fe Kα line profiles are shown in the right panels of the same figure. Taking into account that the gap is formed in the accretion disk around the primary, and for the sake of simplicity, we expressed its radii in the units defined by gravitational radius

$R_g = R_{g1}$ (and mass) of the primary SMBH, in which the both gaps from the left panels of Fig. 5 have the widths of 5 R_{g1}. On the other hand, the gap width can be also expressed in different units of gravitational radius R_{g2} for the secondary SMBH (or equivalently, in terms of its mass), assuming that it is twice as large as the outer radius of the accretion disk around the secondary, for which we adopted the value of 50 R_{g2}, as previously mentioned. Under these assumptions: 5 R_{g1} = 100 R_{g2}, resulting with the following value for the mass ratio of the SMBHB: $q = \dfrac{R_{g2}}{R_{g1}} = 0.05$, as well as with the mass of the secondary SMBH of $M_2 = 2.5 \times 10^7\ M_\odot$. Therefore, this SMBHB has an order of magnitude lower mass ratio than the previously described model, but which is still significantly larger than the limit of $q = 10^{-4}$ below which the secondary SMBH is not able to open a gap in the disk around the primary (see e.g. McKernan et al., 2013, for more details). Another important difference between these two models is an assumption that in the latter case, there is no Fe Kα line emission from the gap, i. e. that the "minidisk" around the secondary SMBH (which is embedded in the gap) gives a negligible contribution to the total line emission of the binary. Such scenario is preferable, although one cannot completely exclude a possibility that some gas can enter the gap and feed a "minidisk" around the secondary which, as a consequence, could create some additional Fe Kα line emission (see McKernan et al., 2013, and references therein).

It can be seen from Fig. 5 that in such a case an empty annular gap in the accretion disk around primary could have significant influence on the resulting line shape, inducing the appearance of the similar ripples as in the case of the first SMBHB model, which is in good agreement with the results of some previous studies (see e.g. McKernan et al., 2013). However, these ripple effects in the second SMBHB model, besides having the lower amplitudes, strongly depend only on the positions and widths of empty gap (or in other words, on its radii), but they do not noticeably vary with time (or orbital phase), since we assumed that the inner and outer radii of the gap are also time independent. In reality, on the other hand, the secondary SMBH would slowly spiral down towards the primary, so the radii and width of empty gap would also change with time, inducing a slow time variability of the resulting ripple effects.

4. Discussion

As it was shown in the previous section, both studied SMBHB models predict occurrences of the ripples in the cores of emitted Fe Kα line profiles. Thus, an important related issue is the possibility to detect such effects in the observed spectra of SMBHB candidates using nowadays and future X-ray detectors, which depends on their spectral resolution and signal-to-noise ratio (S/N).

The presented simulated line profiles were calculated over 200 bins of width $\Delta E = 0.064$ keV, which corresponds to the spectral resolution of $E/\Delta E = 100$

at 6.4 keV. On the other hand, the spectral resolutions of some modern X-ray observatories are: $E/\Delta E \sim 20-50$ in the case of XMM-Newton, ~ 600 at 6 keV for Suzaku, and $\sim 100-1000$ in 0.1–10 keV range for Chandra. Therefore, the performed simulations provide spectral resolution which is comparable to those of modern X-ray detectors, and according just to this property, the SMBHB signatures in the form of ripple effects in their observed Fe Kα line profiles should be detectable even by nowadays X-ray detectors.

However, this is not achievable yet due to insufficient S/N of the modern instruments. Namely, in the ray-tracing simulations S/N depends on the number of photons emitted from a simulated disk (Milošević et al., 2018), which in our case was 5000×5000. Such a large number of photons in our simulations provides much higher S/N ratio than in the current observations by XMM-Newton and Chandra, which is the main cause for difficult detection of SMBHB signatures in the currently observed line profiles, in spite of similar spectral resolutions. However, the planned future X-ray observatories (like Advanced Telescope for High Energy Astrophysics – ATHENA) will be equipped with high signal-to-noise and high spectral resolution instruments ($E/\Delta E \sim 2800$ in 0.2–12 keV range) and will enable the detection of the SMBHB signatures in the observed Fe Kα line profiles.

5. Conclusions

We simulated the Fe Kα line profiles emitted from the following two models of SMBHBs:

(i) a model in which both primary and secondary SMBHs are surrounded by an accretion disk and they are orbiting around their center of mass, and

(ii) a model in which the secondary SMBH clears an empty gap (or cavity) in the disk around primary.

We can summarize the obtained results of these simulations as follows:

(i) Both models leave detectable ripples in the emitted Fe Kα line profiles which may look like an absorption component in the line profile;

(ii) In the first model, such ripples in the composite line profiles are caused by Doppler shifts due to orbital motion, and depend on:
   - orbital phase of SMBHB (time) and cause the periodical variability of the line shapes,
   - mass ratio between the secondary and primary SMBHs,
   - parameters of the accretion disks (e.g. inclination) around both primary and secondary,
   - Keplerian orbital elements, which could potentially enable reconstruction of the observed radial velocity curves and their fitting with Keplerian orbits (see e.g. Bon et al., 2012, for an example);

(iii) In the second model, these ripples do not significantly change in time, but instead:
  – they depend on the parameters of the disk around the primary (especially on the disk inclination),
  – their amplitudes strongly depend on the width and distance of the empty gap from the central SMBH, and hence they could be used for constraining the mass ratios and separations between the components in this type of SMBHBs;

(iv) Spectral resolutions and, especially S/N, of modern X-ray detectors are not sufficient to study in details such signatures of SMBHBs, however this will be possible with the next generation of X-ray observatories, such as ATHENA.

Acknowledgements. This work has been supported by Ministry of Education, Science and Technological Development of the Republic of Serbia, through the projects: 176003 "Gravitation and the Large Scale Structure of the Universe" and 176001 "Astrophysical Spectroscopy of Extragalactic Objects". The authors would like to thank an anonymous referee for very useful and helpful comments and suggestions which significantly improved the presentation of the paper.

References

Aggarwal, K., et al.: 2019, *Astrophys. J.* **880**, 116

Ballantyne, D. R., Fabian, A. C.: 2005, *Astrophys. J.* **622**, L97

Begelman, M.C., Blandford, R.D., and Rees, M.J.: 1980, *Nature* **287**, 307

Bon, E., Jovanović, P., Marziani, P., Shapovalova, A. I., Bon, N., Borka Jovanović, V., Borka, D., Sulentic, J., Popović, L. Č.: 2012, *Astrophys. J.* **759**, 118

Cadez, A., Fanton, C., Calivani, M.: 1998, *New Astron.* **3**, 647

Event Horizon Telescope Collaboration, Akiyama, K. et al.: 2019, *Astrophys. J.* **875**, L1

Fabian, A. C., Rees, M. J., Stella, L., White, N. E.: 1989, *Mon. Not. R. Astron. Soc.* **238**, 729

Fabian, A. C., Iwasawa, K., Reynolds, C. S., Young, A. J.: 2000, *Publ. Astron. Soc. Pacific* **112**, 1145

Fanton, C., Calivani, M., Felice, F., Cadez, A.: 1997, *Publ. Astron. Soc. Jpn* **49**, 159

Hilditch, R. W.: 2001, *An Introduction to Close Binary Stars*, Cambridge University Press, New York

Jovanović, P., Popović, L. Č.: 2008, *Fortschr. Phys.* **56**, 456

Jovanović, P., Popović, L. Č.: 2009, chapter in the book Black Holes and Galaxy Formation, Nova Science Publishers Inc, Hauppauge NY, USA, 249-294 (arXiv:0903.0978)

Jovanović, P., Borka Jovanović, V., Borka, D.: 2011, *Baltic Astron.* **20**, 468

Jovanović, P.: 2012, *New Astron. Rev.* **56**, 37

Jovanović, P., Borka Jovanović, V., Borka, D., Bogdanović, T.: 2014, *Adv. Space Res.* **54**, 1448

Jovanović, P., Borka Jovanović, V., Borka, D., Popović, L. Č.: 2016, *Astrophys. Space Sci.* **361**, 75

Li, Y.-R., Wang, J.-M., Ho, L.C., Lu, K.-X., Qiu, J., Du, P., Hu, C., Huang, Y.-K., Zhang, Z.-X., Wang, K., and Bai, J.-M.: 2016, *Astrophys. J.* **822**, 4

LIGO Scientific Collaboration and Virgo Collaboration, Abbott, B.P. et al.: 2016, *Physical Review Letters* **116**, 061102

McKernan, B., Ford, K. E. S., Kocsis, B., Haiman, Z.: 2013, *Mon. Not. R. Astron. Soc.* **432**, 1468

Milošević, M., Pursiainen, M., Jovanović, P., Popović, L. Č.: 2018, *Int. J. Mod. Phys. A* **33**, 1845016

Paczynski, B.: 1977, *Astrophys. J.* **216**, 822

Planck Collaboration, Aghanim, N. et al.: 2018, *arXiv:1807.06209*

Popović, L. Č.: 2012, *New Astron. Rev.* **56**, 74

Reynolds, C. S.: 2014, *Space Science Reviews* **183**, 277

Safarzadeh, M., Loeb, A., Reid, M.: 2019, *Mont. Not. Royal Astron. Soc.* **488**, L90

Sesana, A., Roedig, C., Reynolds, M.T., and Dotti, M.: 2012, *Mon. Not. R. Astron. Soc.* **420**, 860

Sesana, A., Haiman, Z., Kocsis, B., and Kelley, L.Z.: 2018, *Astrophys. J.* **856**, 42

Shakura, N. I., Sunyaev, R. A.: 1973, *Astron. Astrophys.* **500**, 33

Yan, C.-S., Lu, Y., Dai, X., Yu, Q.: 2015, *Astrophys. J.* **809**, 117

Yu, Q., and Lu, Y.: 2001, *Astron. Astrophys.* **377**, 17